UC Davis
UC Davis Previously Published Works

Title

Conformational changes of the betaine transporter BetP from Corynebacterium glutamicum studied by pulse EPR spectroscopy

Permalink

https://escholarship.org/uc/item/7s61j9ks

Journal

Biochimica et Biophysica Acta, 1818(3)

ISSN

0006-3002

Authors

Nicklisch, SCT
Wunnicke, D
Borovykh, IV
et al.

Publication Date

2012-03-01

DOI

10.1016/j.bbamem.2011.10.021

Conformational changes of the betaine transporter BetP from *Corynebacterium glutamicum* studied by pulse EPR spectroscopy

S.C.T. Nicklisch [a],*, D. Wunnicke [b], I.V. Borovykh [b], S. Morbach [a], J.P. Klare [b], H.-J. Steinhoff [b], R. Krämer [a]

[a] Institute of Biochemistry, University of Cologne, 50674 Cologne, Germany
[b] Department of Physics, University of Osnabrück, 49076 Osnabrück, Germany

ABSTRACT

The betaine transporter BetP from *Corynebacterium glutamicum* is activated by hyperosmotic stress critically depending on the presence and integrity of its sensory C-terminal domain. The conformational properties of the trimeric BetP reconstituted in liposomes in the inactive state and during osmotic activation were investigated by site-directed spin labeling and electron paramagnetic resonance (EPR) spectroscopy. Comparison of intra- and intermolecular inter spin distance distributions obtained by double electron–electron resonance (DEER) EPR with the crystal structure of BetP by means of a rotamer library analysis suggest a rotation of BetP protomers within the trimer by about 15° as compared to the X-ray structure. Furthermore, we observed conformational changes upon activation of BetP, which are reflected in changes of the distances between positions 545 and 589 of different protomers in the trimer. Introduction of proline at positions 550 and 572, both leading to BetP variants with a permanent (low level) transport activity, caused changes of the DEER data similar to those observed for the activated and inactivated state, respectively. This indicates that not only displacements of the C-terminal domain in general but also concomitant interactions of its primary structure with surrounding protein domains and/or lipids are crucial for the activity regulation of BetP.

© 2011 Elsevier B.V. All rights reserved.

1. Introduction

Osmotic stress is one of the most common stress situations which bacteria face in their natural habitat. Under conditions of hyperosmotic stress, the uptake of compatible solutes is one of the first responses by bacteria to counteract water efflux and thus dehydration of the cell [1]. Beside the ABC transporter OpuA from *Lactococcus lactis* [2,3] and the MFS (major facilitator superfamily) carrier ProP from *Escherichia coli* [4,5] the secondary transporter BetP from *Corynebacterium glutamicum* is one of the best studied osmoregulated uptake systems to date [6–9]. Upon the decrease of the external water activity, BetP is activated in less than 1 s and imports its specific substrate glycine betaine in symport with two sodium ions to restore and stabilize the essential cell turgor. BetP is an integral membrane protein with 595 amino acids forming 12 transmembrane helices, which harbor a negatively charged N-terminal domain of approximately 62 amino acids and a positively charged C-terminal domain of about 55 amino

acids, both facing the cytoplasm. Former investigations of the isolated protein reconstituted in proteoliposomes from *E. coli* lipid revealed that BetP is able to directly sense osmotic stimuli, and to respond with modulating its catalytic (transport) activity according to the extent of osmotic stress [10]. Extensive truncation and amino acid replacement studies of BetP heterologously expressed in *E. coli* cells or reconstituted in *E. coli* lipids demonstrated that the integrity, the relative orientation, as well as the fine structure of the C-terminal domain are essential for the osmoregulatory properties of BetP (Fig. 1) [6,8,9]. Despite the detailed knowledge about the regulatory behavior of BetP in relation to ion stimuli [11], membrane composition [9] and the integrity of the terminal domains [6], the molecular mechanism of the activation process is still unknown. The structures of BetP determined by 2D electron [12] and 3D X-ray crystallography [13] proved a trimeric organization of the carrier in the functional state. Thereby, the three monomers form a central conical cavity with hydrophobic residues facing the center. Cavity and the interstitial clefts between the monomers are most likely filled with lipids [13]. The substrate pathway in BetP consists of a narrow, partially hydrophobic lumen with the glycine betaine binding site that can be exposed to either side of the plasma membrane during the activation cycle forming hydrophilic periplasmic or cytoplasmic vestibules [14]. On the basis of these data, certain inter- and intramolecular C-domain/protein and/or C-domain/lipid interactions were suggested to play a key role during the hyperosmotic stress-induced activation of BetP. In particular, it was shown, that the C-domains of each protomer are in direct
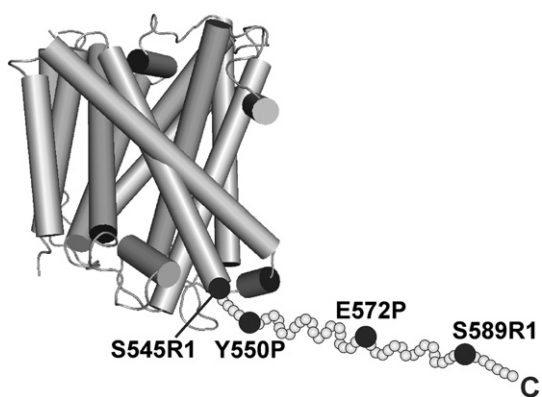
Fig. 1. Structure of the N-terminally truncated glycine betaine carrier BetP from *Corynebacterium glutamicum*. The X-ray structure of protomer A [13] in side view was complemented with a cartoon representation of the C-terminal domain. A bubble spiral between residues 550 and 589 is indicated to depict the region of a known α-helical stretch according to Ott et al. 2008 and Ressl et al. 2009 [6,13]. Highlighted circles illustrate the introduced cysteine and proline residues in the constructs used for EPR measurements.

contact with cytosolic loops of the adjacent subunit and thus may act as an allosteric switch between neighboring protomers [13,14].

The current model for the activation process of BetP involves a complex C-domain/N-domain/phospholipid interaction in the resting state of the transporter [6]. Upon the stress-induced activation of BetP, a switch-like movement of the C-domain towards the protein environment was assumed to occur. In addition, it has to be taken into account that BetP is a functional trimer, and the oligomeric state may be relevant for osmosensing and/or osmoregulation as well [12,13]. We were interested in the conformation and in conformational changes of the C-terminal domain of BetP or of domains in the close vicinity to the C-terminal domain upon BetP activation. To further elucidate the dynamic behavior of the C-terminal domain and its significance for the osmosensory and osmoregulatory properties of BetP, we used site-directed spin labeling electron paramagnetic resonance spectroscopy (SDSL EPR) [15–17]. SDSL EPR is an appropriate biophysical strategy for the analysis of challenging membrane proteins [18–20], and has been successfully applied to define secondary and tertiary structure elements of membrane proteins [19,21,22], structural models of membrane proteins [23–25] and to analyze their conformational changes [19,20]. For this purpose, we constructed various BetP mutants with strategically located single cysteine residues at the beginning (S545C) and close to the end (S589C) of the C-domain, as well as a double mutant combining these cysteine replacements (S545C/S589C) (Fig. 1). After spin labeling we used these recombinant forms of BetP for monitoring structural changes by continuous wave and pulse EPR spectroscopy. The combination of local and global information derived from these studies reveals insights into the structural properties of the membrane-embedded BetP trimer and provides direct experimental evidence for a conformational change upon activation, which involves the C terminus.

2. Materials and methods

2.1. Bacterial strains and plasmids

The generation of single cysteine BetP variants was done by site-directed mutagenesis using the cysteine-free BetP mutant C252T as PCR template [10], two synthetic oligonucleotide primers containing the desired point mutation as well as the proof-reading *PfuTurbo®* DNA polymerase which replicates both plasmid strands without displacing the mutant primers. In the following the PCR product was treated with the endonuclease *Dpn I* that specifically digests the methylated, nonmutated parental DNA template, and transformed into supercompetent *E. coli* DH5α (*endA1 supE44 thi-1λ⁻ recA1 gyrA96 relA1 deoR Δ(lacZYA-argF) U169 Φ80dlacZ ΔM15 mcrA Δ(mrr hsdRMS mcrBC)*) cells via heat shock transformation [26]. Clones were verified by DNA sequencing.

2.2. Expression and growth conditions

For heterologous overexpression, the respective *betP* gene was cloned into the vector pASK-IBA5 (IBA GmbH, Göttingen, Germany), in which *Strep-betP* is under the control of the *tetA* promotor. *E. coli* DH5α (*endA1 supE44 thi-1λ⁻ recA1 gyrA96 relA1 deoR Δ(lacZYA-argF) U169 Φ80dlacZ ΔM15 mcrA Δ(mrr hsdRMS mcrBC)*) cells were then transformed with the resulting plasmid. Cells were grown at 37 °C in LB medium and supplemented with carbenicillin (50 μg/ml). Induction was carried out in exponentially growing cells ($OD_{600} = 0.9$) upon the addition of 200 μg anhydrotetracycline/liter cell culture.

2.3. Protein purification and preparation of proteoliposomes

Membranes were prepared by threefold high pressure cell disruption in a French Press (Thermo Electron Corporation, Needham Heights, USA) and subsequently with differential centrifugation for 30 min at 12,000 g (cell debris) and for 45 min at 210,000 g (membranes) at 4 °C. Membranes were suspended in 50 mM KPi (pH 7.5), 8.6% glycerol, 1 mM EDTA. Solubilization was performed by dropwise addition of 2% DDM (w/v) and incubation for 30–60 min at 4 °C. Residual membranes were separated by centrifugation for 20 min at 86,900 g and 4 °C, and the supernatant was diluted 1:4 with 50 mM KPi (pH 7.5), 200 mM NaCl, 8.6% glycerol, 1 mM EDTA. Strep-tagged BetP was solubilized and purified by *Strep tag II* affinity chromatography (IBA, Göttingen, Germany). Prior to column application, the Strep-Tactin resin (5 ml Strep-Tactin MacroPrep, IBA, Göttingen, Germany) was equilibrated by adding 5 column volumes of low-salt buffer (50 mM KPi, pH 7.5, 200 mM NaCl, 1 mM EDTA, and 8.6% glycerol, 0.1% DDM). Subsequent to the application, two washing steps with high-salt (50 mM KPi, pH 7.5, 500 mM NaCl, 1 mM EDTA, 8.6% glycerol, 0.1% DDM) and low-salt buffer were carried out.

From a standard cultivation, we obtained 1–1.5 mg of highly pure *Strep*-BetP/liter of cell culture. Protein concentration determination was carried out using the Amido Black method [27]. For reconstitution, liposomes (2 mg/ml phospholipids) prepared from phospholipids of *E. coli* polar lipid extract (Avanti Polar Lipids, Inc., Alabaster, AL) were preformed by extrusion (19 cycles) through polycarbonate filters (400 nm pore size). To confirm saturation of the liposomes with detergent, light scattering measurements at OD_{540} were performed upon the stepwise addition of 20% Triton X-100. Solubilized BetP was added at a lipid-to-protein ratio of 20:1 (w/w) and incubated for 30 min at room temperature. To remove excess detergent, a combination of dialysis and hydrophobic adsorption onto Bio-Beads (Biorad, Munich, Germany) was used (see supplemental materials for details). Finally, proteoliposomes were centrifuged, washed in 100 mM KPi (pH 7.5) and concentrated to yield a BetP concentration of 50–100 μM (100 μM = 6.42 mg/ml). Proteoliposomes were frozen in liquid N_2 and stored at −80 °C until use. Quantitative depletion of the major detergent constituent DDM was tested using an optical assay. Therefore, the DDM maltoside moiety was cleaved with yeast maltase (Sigma-Aldrich Chemie GmbH, Munich, Germany). The resulting glucose was phosphorylated and determined in an optical test using G6P dehydrogenase. For further details concerning BetP reconstitution into liposomes see supplementary material, section 1.

2.4. Spin labeling

Spin labeling of BetP and pretreatment with the reducing agent dithiothreitol (DTT) were performed with the DDM-solubilized protein bound to the affinity column. The thiol groups were reduced with 10 mM DTT for 3 h at 4 °C and washed with degassed low-salt buffer (see above). The reaction with the MTS nitroxide spin label ((1-Oxyl-2,2,5,5-tetramethylpyrrolidin-3-yl) methyl-methanethiosulfonate, Toronto Research Chemicals, Toronto) was carried out with a spin label-to-protein ratio of 10:1 (M/M) overnight at 4 °C. Unbound spin label was removed by washing with 10 column volumes of low-salt buffer and 0.1% DDM. Labeled BetP was eluted with 50 mM KPi (pH 7.5), 200 mM NaCl, 1 mM EDTA, 8.6% glycerol, 0.1% DDM and 5 mM desthiobiotin (Sigma-Aldrich Chemie GmbH, Munich, Germany). The labeling efficiencies have been determined to be in the range of ~40–90%.

2.5. Determination of proteoliposomal leakage and BetP orientation

To determine leaky lipid vesicles prior to the measurements and/or to quench superimposing signals of proteoliposomes with wrongly (inside-out) orientated BetP, we applied two different assays. The integrity of BetP-R1 proteoliposomes after Bio-Bead/dialysis reconstitution was determined by an optical quenching method using the fluorophore calcein [28]. Proteoliposomes were slowly thawed at room temperature and collected by ultracentrifugation. 30 mM calcein (Sigma-Aldrich, Munich, Germany) was diluted in 100 mM KPi, pH 7.5. The pH value of the calcein solution was adjusted to 7.2 by stepwise addition of 1 M KOH. Proteoliposomes were then suspended in the calcein solution and extruded 19 times through polycarbonate filters (pore diameter 400 nm). External calcein was removed by three gel filtrations using G75 sepharose (GE Healthcare, Munich, Germany) columns. Fluorescence measurement was carried out with an Aminco Bowman Series 2 Spectrometer (SLM Aminco, Büttelborn, Germany) at an excitation wavelength of 495 nm and an emission wavelength of 520 nm (slit width of 8 nm). Free calcein migrated slowly as a yellow fluorescent band through the column resin while the proteoliposomes with self-quenching internal concentrations of calcein (30 mM) could be eluted first as an orange-colored band in 1–2 ml 100 mM KPi buffer, pH 7.5. All orange-colored samples were kept at RT for about 3–4 h and subjected to another gel filtration to measure the occurrence of leaked out calcein. If free calcein was detected, the proteoliposomes were subjected to another Biobead/Dialysis cycle and/or fused with *E. coli* lipids to restore their integrity.

A more convenient method to test both, the integrity of proteoliposomes with incorporated, spin labeled BetP and its orientation was performed by the addition of a water soluble spin relaxant (50 mM chromium-(III)-oxalate (CrOx, $Cr(C_2O_4)^{3-}$), Sigma-Aldrich, Munich, Germany) to the external buffer, thus quenching the EPR signal [29]. The addition of the membrane impermeable quencher leads to a signal decrease proportional to the amount of inside-out orientated, spin labeled BetP and of spin labeled BetP incorporated in leaky liposomes. With this method it was possible to estimate the correct protein incorporation online during the EPR measurements (see supplementary Fig. S3).

2.6. Transport assays

Transport activity measurements with proteoliposomes were performed upon increasing the osmolality of the buffer (100 mM KPi, pH 7.5) by addition of external solutes. In the assays used, K^+ is the predominant luminal cation present. Accordingly, the internal K^+ concentration increases from approximately 200 mM to 500 mM, when the applied external osmotic upshift changes from 200 to 1000 mM [30]. Consequently, BetP is activated with half-maximum of activation around 200 mM K^+. The impact of each amino acid substitution and modification on BetP activity was analyzed in proteoliposomes.

After thawing, proteoliposomes were extruded 19 times through a polycarbonate filter (400 nm pore size, Whatman Inc., Newton, USA) at room temperature in 100 mM KPi (pH 7.5), collected by centrifugation and resuspended in the buffer to a lipid concentration of ~60 mg/ml lipid. An appropriate amount of proteoliposomes with ~2–2.5 μg/μl BetP was diluted 200-fold in 50 mM NaPi (pH 7.5) containing 15 μM [^{14}C] glycine betaine and 0.5 μM valinomycin to create an outwardly directed K^+ diffusion potential. To establish hyperosmotic conditions, proline (for EPR measurements under hyperosmotic conditions also NaCl and KCl were used) was added to the external medium. The uptake measurements were started with the addition of proteoliposomes. Samples were taken and rapidly filtered through 0.22 μm GS nitrocellulose filters (Millipore Corp., Eschborn, Germany) after 5 and 10 s. The filters were washed with 100 mM LiCl, and the radioactivity was determined by liquid scintillation counting.

2.7. EPR spectroscopy

Room temperature continuous wave (cw) X-band EPR spectra were recorded using a MiniScope MS200 spectrometer (Magnetech). For cw measurements, about 15–20 μl of the sample was loaded into glass capillaries with 0.9 mm inner diameter. To avoid saturation and to obtain high signal-to-noise ratio EPR spectra were taken at the microwave power set between 1 and 5 mW. The B-field modulation amplitude was set between 1 and 2 G depending on the width of the sharpest EPR line.

Pulse EPR experiments (DEER) were performed at X-band frequencies (~9.3 GHz) on a Bruker Elexsys 580 spectrometer equipped with a Bruker Flexline split-ring resonator ER 4118X-MS3 and a continuous flow helium cryostat (ESR900; Oxford Instruments) controlled by an Oxford Intelligent temperature controller ITC 503S. 40–50 μl of the sample was loaded into glass capillaries with 2.4 mm inner diameter. All measurements were performed at 50 K using the four-pulse DEER sequence [31, 32]: $\pi/2\ (\upsilon_{obs}) - \tau_1 - \pi\ (\upsilon_{obs}) - t' - \pi\ (\upsilon_{pump}) - (\tau_1 + \tau_2 - t') - \pi\ (\upsilon_{obs}) - \tau_2 -$ echo. A two-step phase cycling $(+\langle x\rangle, -\langle x\rangle)$ was performed on $\pi/2\ (\upsilon_{obs})$. Time t' is varied, whereas τ_1 and τ_2 are kept constant, and the dipolar evolution time is given by $t = t' - \tau_1$. Data were analyzed only for $t > 0$. The resonator was overcoupled to Q ~ 100; the pump frequency υ_{pump} was set to the center of the resonator dip and coincided with the maximum of the nitroxide EPR spectrum, whereas the observer frequency υ_{obs} was 65 MHz higher, coinciding with the low field local maximum of the spectrum. All measurements were performed at a temperature of 50 K with observer pulse lengths of 16 ns for $\pi/2$ and 32 ns for π pulses and a pump pulse length of 12 ns. Proton modulation was averaged by adding traces at eight different τ_1 values, starting at $\tau_{1,0} = 200$ ns and incrementing by $\Delta\tau_1 = 8$ ns. The total measurement time for each sample was 4–24 h. Analysis of the data was performed with DeerAnalysis 2008/2009 using Tikhonov regularization [36]. Error analysis (validation) of distance distributions was carried out with the validation tool included in the DeerAnalysis software. For the bounds and number of trials tested with the respective datasets the suggestions the software makes based on the result of the background correction performed, using the setting "Fine grid", have been taken. The parameters varied were the background density and the modulation depth.

2.8. Rotamer library analysis

Distance distributions were simulated using a rotamer library of spin labeled residues as described in [33]. The rotamer library consisted of 98 rotamers of MTSSL bound to cysteine, which have been used to replace the native residues at the positions of interest in the respective BetP structural models (see Results). Energies and resulting populations for individual rotamers were calculated by means of

a Lennard–Jones potential at 175 K, which is the glass transition temperature for a water–glycerol mixture. This temperature most likely reflects the ensemble of spin label conformations obtained by cooling the sample down to 50 K. These populations were then used as weights in the simulation of the distance distributions.

3. Results

3.1. Introduction of cysteine residues at strategic locations within the C-terminal domain

For the analysis of the dynamic properties of the C-terminal domain of BetP, original amino acids at strategic locations, namely at the beginning (amino acid position 545) and close to the end (589) of the C-terminal domain of the BetP-C252T mutant (Fig. 1), were replaced by cysteines and subsequently labeled with MTSSL (in the following the spin label side chain is abbreviated with R1). Based on the predicted protein topology (Fig. 1) and crystal structure [13], position 545 is close to the central conical cavity of the trimer at the beginning of the C-terminal domain. This vestibule as well as the deep clefts between the monomers are supposed to be filled with lipids that may influence the local environment at position 545 of BetP reconstituted in the liposomes (Fig. 5 in [13]). Position 589 is close to the end of the C-terminal domain of BetP (Fig. 1). According to the functional model of BetP activation [6,26], pronounced conformational changes in this region of C-terminal domain would be expected when the carrier is activated.
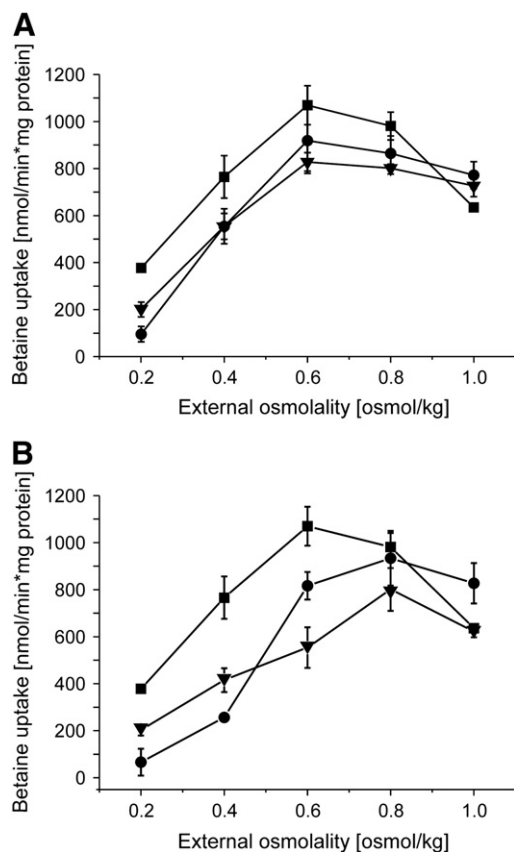
As an essential requirement for further studies, the activity of the two cysteine mutants in proteoliposomes was tested without (Fig. 2A) and with the MTS spin labels bound to the protein (Fig. 2B). Both single mutant forms of BetP showed regulation properties close to the wild type. Interestingly, in both cases the activation optimum slightly shifted to higher osmolalities, from about 600 to about 800 mOsm/kg (Fig. 2B). However, the attachment of the spin label to the selected positions did not impair the transport activity, i.e. a higher uptake rate in response to an increased osmolality. Thus, neither stimulus perception nor signal transduction of these BetP variants was influenced by the spin label attachment. The respective double mutant was also found to be fully osmoregulated in *E. coli* cells (see supplementary Fig. S4).

3.2. Mobility screening upon hyperosmotic stress-induced BetP activation

In order to probe the local structure of the C-terminal domain we analyzed the spin label mobility of the two cysteine mutants of BetP solubilized in detergent and reconstituted in *E. coli* lipid proteoliposomes. A comparison of the spin label mobility before and after reconstitution into *E. coli* liposomes should provide information about C-domain/lipid interactions in the resting state of BetP. Once reconstituted, the induced activation of BetP is thought to be accompanied by a conformational change within the C-domain. Thus, an altered environment for the selected amino acid positions might result in changes of the motional restriction for the attached spin label, thereby visible as changes of the EPR spectral shape. Fig. 3 shows the EPR spectra of the mutants in detergent and in proteoliposomes in the presence and absence of activating amounts of NaCl or proline in the external buffer. In detergent-solubilized BetP, the spin label at position 545 shows broad spectral lines, typical for sites with pronounced mobility restrictions, e.g. at helix/helix interfaces [34]. Contrarily, the spectrum for position 589 at the end of the helix reveals sharp lines for the solubilized state, indicating weak motional restrictions. Reconstitution of the spin labeled BetP mutants into proteoliposomes resulted in broadening of the respective lines, indicating a decrease of the spin label mobility in both cases. Although also
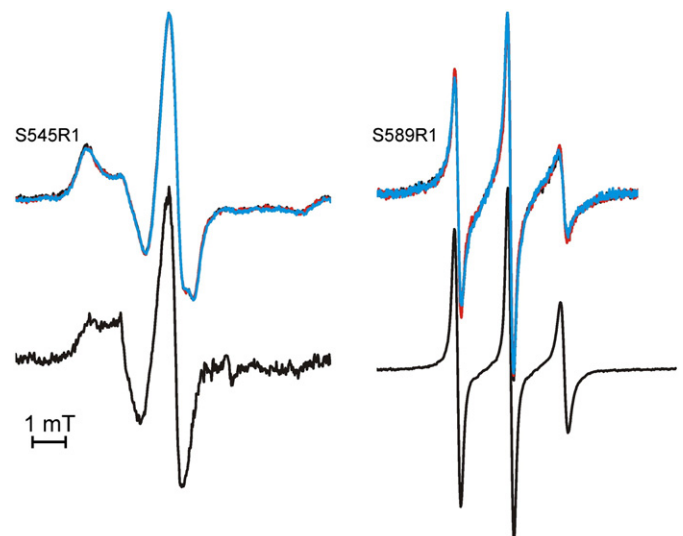

Fig. 2. Activity regulation of BetP-C252T (Cys-less) and BetP variants without (A) and with spin label (B) as function of the external osmolality reconstituted in *E. coli* lipid liposomes. Uptake of ^{14}C-glycine betaine was measured under hyperosmotic conditions (see Materials and methods). The internal buffer contained 100 mM K$^+$-phosphate (pH 7.5) at a total osmolality of 0.22 Osm/kg. The external buffer was composed of 50 mM Na$^+$-phosphate (pH 7.5) at an osmolality of 0.1 Osm/kg. Higher external osmolalities were adjusted by the addition of proline. Each data point represents the mean of five independent measurements. BetP variants: ■ C252T (control), ● S545C, ▼ S589C.

Fig. 3. Cw-EPR spectra of MTS spin label bound to positions 545 and 589 in the C-terminal domain of BetP in proteoliposomes. Top: In the absence (black) and presence of activating amounts of 400 mM NaCl (red) or 800 mM proline (blue) and 40 mM CrOx in the external buffer. Bottom: EPR spectra of the respective detergent solubilized BetP samples. Experimental parameters: modulation amplitude 1 G, time constant 100 ms, microwave power 1 mW, scan time 120 s, temperature stabilized at 20 °C. All spectra are normalized to the amplitude of the center resonance line.

reduced upon reconstitution, the mobility of S589R1 remained significantly higher as compared to that of S545R1.

The EPR spectra of both BetP variants showed very small changes in the spectral line shape upon the addition of activating amounts of NaCl or proline to the external buffer, indicating that possible conformational changes involving the C-terminal domain cause no significant changes of the spin label side chain motional freedom, i.e. that the immediate spin label environment remains unaltered.

3.3. Distance measurements in dependence of the state of BetP activity

As we were not able to observe conformational changes of the BetP C-terminal domain upon activation by analyzing the spin label mobility, we applied double electron–electron resonance (DEER) [33,35] EPR spectroscopy to quantitatively measure intra- and intermolecular distances between spin labeled positions and to study global structural changes during BetP function. The results of the distance measurements are shown in Fig. 4. Pulse EPR measurements with the corresponding DEER analyses of three different batches of BetP-S545R1 in proteoliposomes reproducibly led to a mean distance of 30 ± 4 Å between the individual 545 positions within a reconstituted BetP trimer. The minor distance increase observed upon the addition of activating amounts of NaCl was found to be within the experimental error when comparing different datasets. Smaller peaks in the distance distributions observed at ~45–60 Å turned out to be non-significant as judged by analyses of the data with the build-in validation tool of DeerAnalysis 2008/2009 [36]. The significantly reduced modulation depth for BetP-S545R1 in the activated compared to the non-activated state is caused by a lower spin labeling efficiency for this particular sample. For the terminal position 589 in the activated and in the non-activated state of BetP-S589R1, we could not resolve any spin–spin interactions within the accessible
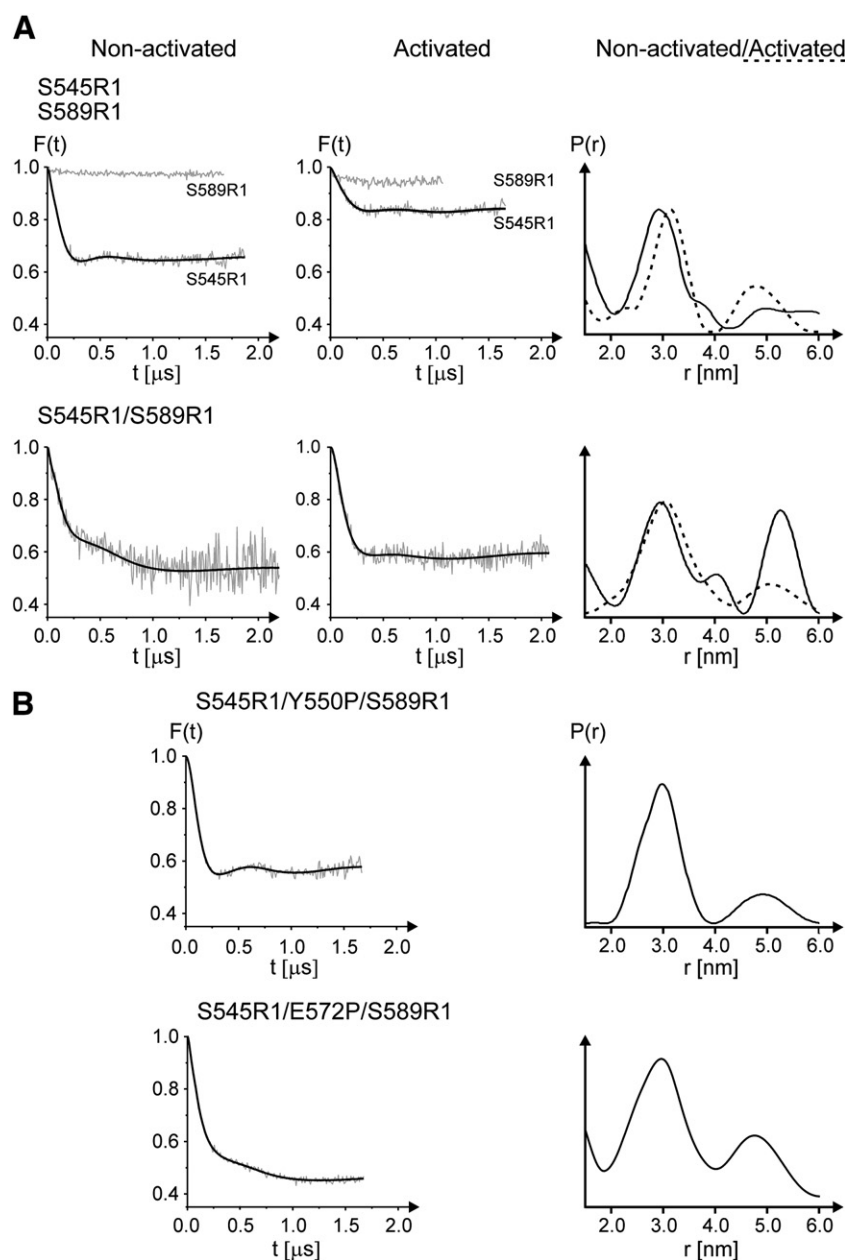

Fig. 4. Results of DEER measurements using single and double cysteine mutants of BetP. The DEER dipolar evolution data, F(t), have been corrected for an exponentially decaying background arising from a three-dimensional distribution of remote spins. The corresponding distance distributions, P(r) are shown in the right column. Each mutant form was measured in proteoliposomes both in the resting (*solid line*) and the activated state (*dashed line*). The absence of any modulation depth in the DEER data obtained with the spin labeled mutant BetP-S589R1 in the activated or non-activated state points to a spin–spin distance far above the sensitivity range of the measurements of ~5 nm.

distance range (Fig. 4A, F(t) in the upper left and central panel). Consequently, the intermolecular distances between spin labels attached to position 589 are >45 and >40 Å for non-activated and activated BetP, respectively.

The reconstituted double mutant with spin labels bound to positions 545 and 589 (BetP-S545R1/S589R1) again revealed a mean distance of about 30 ± 3 Å, resulting from the spin–spin interaction between the 545 positions. Noteworthy, distance measurements performed on detergent-solubilized BetP-S545R1 and BetP-S545R1/S589R1 revealed also short-distance peaks at ~29 ± 3 Å and 28 ± 5 Å, respectively (see supplementary Fig. S5), which are attributable to the intermolecular S545R1 pair interactions within the trimer.

In the double mutant BetP-S545R1/S589R1, distance contributions in the >40 Å range turned out to be significant as the complete set of possible distance distributions obtained from the validation procedure exhibits a non-zero probability to find contributions in this distance range (Fig. 4A, lower panels). However, it is not possible to define the exact position and width of this long-distance peak due to the limited length of the dipolar evolution trace. In the activated state, this long-distance contribution is strongly decreased as is obvious from a direct comparison of the respective dipolar evolution traces, F(t), in the region from ~0.2 to 1.0 μs (Fig. 4A, lower panels). This is clear evidence for a conformational change taking place upon activation.

In order to study the possible influence of C-domain displacement on the interspin distance distributions, we constructed two different proline mutants with a single proline substitution right ahead (BetP-S545R1/Y550P/S589R1) or in the center (BetP-S545R1/E572P/S589R1) of a known α-helical stretch within the C-domain [6,13]. The proline replacements are assumed to introduce a 'proline-kink' at different sites, which are supposed to alter the intra- and inter-protomer 545–589 distances to different extents (cf. Fig. 5A). The insertion of the proline residues leads to a permanent transport activity of BetP at a low level (see supplementary Fig. S4 and [6] for details). Both the proline replacements did not affect the 30 Å peak in the distance distribution, but revealed differences in the DEER traces corresponding to differences in the long distance peak >40 Å, which have also been proven to be significant. Based on these findings we assign the changes observed in the distance peak >40 Å (Fig. 4A), to changes of the intra- and inter-protomer 545–589 distances in the trimer.

3.4. Comparison of the DEER data with structural models of the BetP trimer

The distance distributions obtained by DEER spectroscopy were compared with the structural model for the BetP trimer obtained by X-ray crystallography [13] by means of a rotamer library analysis (RLA, see Materials and methods) for positions 545 and 589. For the initial analysis we took the crystal structure (PDB ID: 2WIT) and used the single fully resolved C-terminal helix (see Fig. 5, Monomer A in [13]) to complete the other two (partially resolved) helices in the respective orientations as present in the crystal structure (Fig. 5A). The result of the analysis for BetP-S545R1/S589R1 is shown in comparison with the experimental DEER distance distribution for this mutant (non-activated) in Fig. 5B. The calculated distance distributions seem to deviate from the experimental data. Especially, the mean distances calculated between the nitroxides of S545R1 in the trimer are 6–8 Å larger than the experimental ones. In addition, none of the other possible spin label pairs (545–589 and 589–589 in different combinations in the trimer) yields distance values which would resemble the distance peak at ~45–60 Å in the experimental data. Nevertheless, the widths of the peaks in the distance distributions compare quite well between calculation and experiment, indicating that the conformational space accessible for the spin label side chain is satisfactorily reproduced by the RLA. To check if variations of the orientation of the C-terminal helices can lead to a distance

distribution as found in the EPR experiment we completely removed the helices to release any strain on the spin label conformational space and again calculated the distance distributions for positions 545. It turned out, that even in this case the conformational space accessible for the spin label side chain does not sufficiently include the
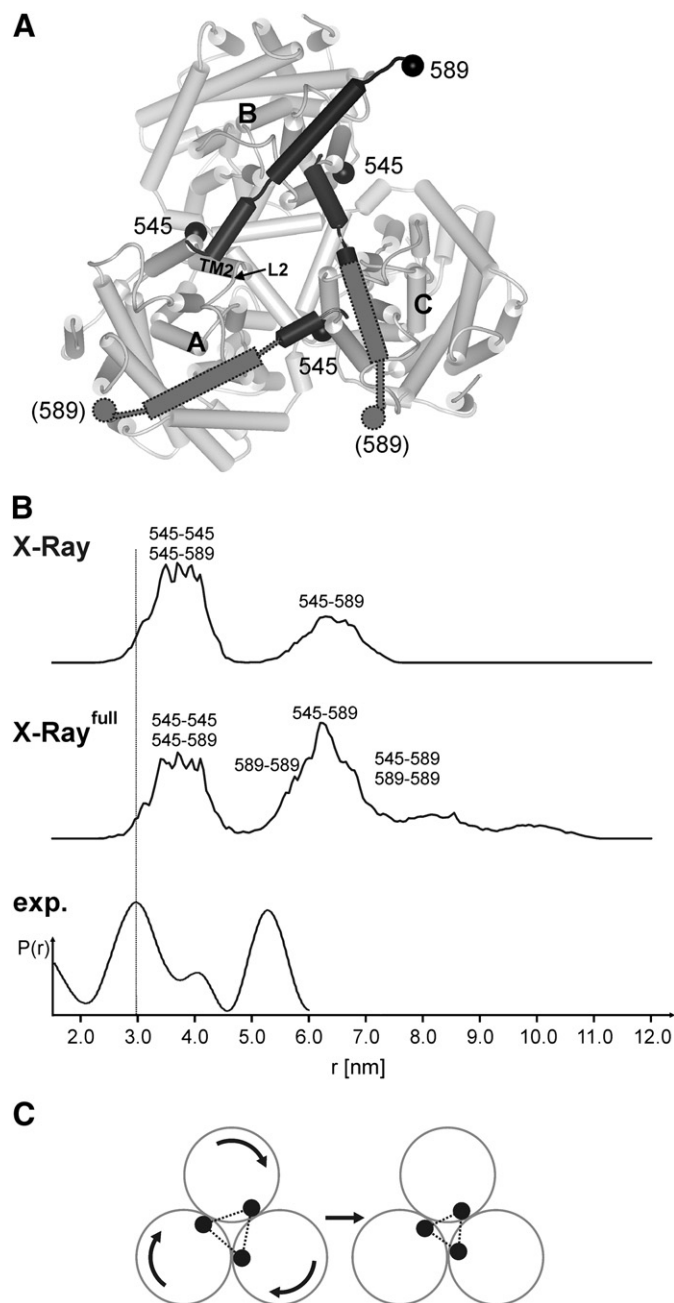

Fig. 5. Rotamer library analysis for the BetP trimer. (A) X-ray structure of the BetP with a periplasmic view on the trimer and its α-helices in cylindrical presentation (PDB ID: 2WIT) [13]. The C-terminal parts (shown in dark gray) of two of the protomers are not resolved in the crystal structure. To allow a full rotamer analysis (X-ray^{full}) in (B) the two missing parts have been complemented with the structure of the fully resolved C-terminal helix of protomer A (gray boxes with dotted frames represent the helical parts, residues given in brackets). Residues S545 and S589 are indicated as black balls at the positions of their respective Cα atoms. (B) Calculated distance distributions form the crystal structure (X-ray) and from the crystal structure complemented with the two C-terminal domains (X-ray^{full}) are compared to the experimental (exp.) distance distribution of BetP-S545R1/S589R1 (non-activated). The intra- and intermolecular spin label pair contributions to the calculated distance distributions are indicated by their residue numbers. (C) Suggested rotation of the BetP subunits within the trimer to bring positions 545 in closer proximity (see text).

distance range found in the experiment. We therefore conclude that changes in the core of the BetP trimer with respect to the crystal structure are necessary rather than a reorientation of the C-terminal helices alone to explain the experimental results for BetP in liposomes. If we assume that the packing of the proteins in the trimer but not the core structure of the single BetP units differs from the crystal structure a rotation of the BetP protomers by about 15° (Fig. 5C) leads to a relative displacement of the 545 positions that results in a calculated distance distribution which satisfactorily reproduces the experimental one not only in the 30 Å region but also for the distance range > 45 Å.

4. Discussion

In order to probe the local structure of the C-terminal domain of BetP as well as putative structural changes induced by BetP activation, we constructed site-directed mutants of BetP carrying single or double cysteine replacements within the C-terminal domain and applied site-directed spin labeling in combination with EPR spectroscopy. The results obtained by screening the mobility of the spin label side chains indicated a strengthening of the interaction between the C-terminal domain of BetP with adjacent structures upon reconstitution into proteoliposomes. In particular, the mobility of S545R1 was strongly restricted upon membrane incorporation. Based on the X-ray structure [13] the spin label at position 545 is located near the proximal end of the C-terminal domain in close vicinity to the monomer–monomer clefts in the BetP trimer that may in general adapt a more rigid structure upon reconstitution into lipids [13]. Also the mobility of the spin label bound to position 589 decreases upon membrane reconstitution but is still significantly higher than that observed for position 545. In the X-ray structure the C-terminal domain seems to directly interact with or even bind to other protein domains of adjacent protomers in the BetP trimer [13]. The observed mobility decrease of S589R1 indicates that the C-terminal domain weakly interacts either with other domains of BetP or with the lipid bilayer, the latter being in line with a suggested functional model [6,37] in which the C-terminal domain is supposed to interact with the surrounding phospholipid headgroups in the resting state. However, the slight upshift of the activation optimum observed upon introduction of a spin label side chain at either position might indicate an interaction with other BetP domains [14]. A shift of sensitivity in the same direction but to a much larger extent has been observed for mutants with a truncated N-terminal domain [38]. The N-terminal domain is supposed to interact with the central part of the C-terminal domain of BetP [6]. Consequently, such a sensitivity shift might indicate an interference with the functional contact between the two terminal domains.

According to the present data the C-terminal domain is characterized by high flexibility which would be in agreement with its putative function as a molecular switch [6]. Nevertheless, osmotic stress induced activation did not alter the overall spin label mobility as would be expected for a 'molecular switch' movement of the whole C-terminal domain as suggested in the above mentioned model. At first glance, this would indicate that the secondary structure of the C-terminal domain as well as the local environment of the investigated spin label side chains do not significantly change upon BetP activation. On the other hand, a recent publication on conformational changes of the G-protein-coupled receptor rhodopsin demonstrated that global structural changes may remain undiscovered by analyzing changes of the spin label mobility only. Unlike spectral shape analysis, distance measurements using the DEER technique revealed a distinct outward tilt of the TM6 helix of rhodopsin during photoactivation [39]. Thus, to analyze the structural properties of the C-terminal helices and possible conformational changes upon activation, we carried out distance measurements using single and double spin labeled BetP variants as well as triple mutants harboring an additional proline

in the C-terminal domain. Based on the defined spin–spin distance of 30 Å for positions 545 within the BetP trimer, the proximal end of the C-terminal domain of each protomer within the functional trimer was confirmed to be orientated near to the core region of the trimer (Figs. 4A and 5A). Nevertheless, a comparison of the experimental distance value with calculated distance distributions based on the published BetP trimer structure [13] revealed that the core structure of the trimer in liposomes seems to differ from that in the crystal. Assuming that the structure of the protomers is less affected by the environment in the crystal than their packing in the trimer, we find that a clockwise rotation (if seen from the cytoplasm) of the BetP monomers (Fig. 5C) leads to a calculated distance distribution which resembles the experimental data. Such rotation appears to be necessary as S545 is oriented nearly perpendicular with respect to the line connecting $C\beta^{545}$ with the threefold symmetry axis, and TM2 and L2 of the respective protomer prevent orientations of the spin label side chain necessary to yield the experimentally observed interspin distances. Alternatively we have to assume that TM2 and L2 in each of the BetP monomers in liposomes have to be shifted with respect to their positions found in the crystal structure that would lead to the required rotation of TM12, where S545 is located. Influences of lipids on the distance distributions due to modulation of the accessible space for the spin label side chain cannot be excluded; however, this does not affect the lower distance limit in the 545–545 distance distributions given by the sterical interaction of the spin label with TM2 and L2.

Positions 589 within the three protomers of the BetP-trimer were too far apart from each other to be measurable within the sensitivity range of the experimental setup, i.e. the intermolecular distance must exceed 40–45 Å. Indeed, our rotamer library analysis shows that the expected interspin distances in this case are ~75–100 Å. This result clearly shows that under *in vivo* conditions the distal ends of the C-terminal domains must be exposed to the exterior of the BetP trimer and are not in close vicinity. DEER analysis of the double mutant S545R1/S589R1 revealed, in addition to the 30 Å distance, inter spin distances in the > 45 Å range. Also for these distance distributions, agreement between the experimental and the calculated distributions can be achieved, if the packing in the trimer resembles that of the model (Fig. 5C) suggested here. Alternatively, bending of the C-terminal helices would shift the calculated interspin distances closer to the experimental values.

Analysis of the data for BetP in the activated state do not reveal any significant changes in the distance between positions 545 upon activation, indicating that neither large-scale conformational changes at the attachment point of the C-terminal domain, i.e. the cytoplasmic end of TM12, nor significant rotations of the protomers within the trimer take place. In contrast, for the double mutant S545R1/S589R1, a depletion of the 45–55 Å distance peak, which has been assigned to intra- and inter-protomer 545–589 interactions, is observed. Remarkably, the introduction of a proline right ahead of the α-helical stretch (Y550P) led to changes in the distance distribution, which are similar to those observed upon activation (cf. Fig. 4A lower panels and B). This suggests that the conformational changes observed for the C-terminal domains upon activation might be similar to those induced by insertion of a proline at position 550, being in line with the observation that this mutant is characterized by a permanent transport activity, however, at a low level [6]. Strikingly, the DEER trace, F(t), obtained for the variant with a proline at position 572 in the center of the helix, which also leads to a permanent transport activity at low level, resembles that of non-activated BetP. Consequently, a distinct displacement of the C-domain seems to be necessary but not sufficient for correct stimulus sensing and/or signal transduction during BetP function. The question, however, whether and to what extent additional interactions of the C-terminal domain with cytoplasmic loops or the N-terminal domain of the adjacent protomers might be modulated upon activation is still under debate and

might be unraveled by future DEER-EPR investigations such as C-domain/N-domain/internal loop triangulation experiments.

Acknowledgements

Appendix A. Supplementary data

Supplementary data to this article can be found online at doi:10. 1016/j.bbamem.2011.10.021.

References

[1] J.M. Wood, Osmosensing by bacteria: signals and membrane-based sensors, Microbiol. Mol. Biol. Rev. 63 (1999) 230–262.

[2] E. Biemans-Oldehinkel, M.K. Doeven, B. Poolman, ABC transporter architecture and regulatory roles of accessory domains, FEBS Lett. 580 (2006) 1023–1035.

[3] T. Van der Heide, B. Poolman, Osmoregulated ABC-transport system of *Lactococcus lactis* senses water stress via changes in the physical state of the membrane, Proc. Natl. Acad. Sci. U. S. A. 97 (2000) 7102–7106.

[4] D.E. Culham, B. Lasby, A.G. Marangoni, L.J. Milner, A.B. Steer, R.W. van Nues, J.M. Wood, Isolation and sequencing of *Escherichia coli* gene *proP* reveals unusual structural features of the osmoregulatory proline/betaine transporter ProP, J. Mol. Biol. 229 (1993) 268–276.

[5] J.M. Wood, Osmosensing by bacteria, Sci. STKE 17 (2006) 43–47.

[6] V. Ott, J. Koch, K. Späte, S. Morbach, R. Krämer, Regulatory properties and interaction of the C- and N-terminal domains of BetP, an osmoregulated betaine transporter from *Corynebacterium glutamicum*, Biochemistry 47 (2008) 12208–12218.

[7] H. Peter, A. Burkovski, R. Krämer, Isolation, characterization and expression of the *Corynebacterium glutamicum betP* gene, encoding the transport system for the compatible solute glycine betaine, J. Bacteriol. 178 (1996) 5229–5234.

[8] D. Schiller, R. Rübenhagen, R. Krämer, S. Morbach, The C-terminal domain of the betain carrier BetP of *Corynebacterium glutamicum* is directly involved in sensing K^+ as an osmotic stimulus, Biochemistry 43 (2004) 5583–5591.

[9] D. Schiller, V. Ott, R. Krämer, S. Morbach, Influence of membrane composition on osmosensing by the betaine carrier from *Corynebacterium glutamicum*, J. Mol. Biol. 281 (2006) 7737–7746.

[10] R. Rübenhagen, H. Rönsch, H. Jung, R. Krämer, S. Morbach, Osmosensor and osmoregulators properties of the betaine carrier BetP from *Corynebacterium glutamicum* in proteoliposomes, J. Biol. Chem. 275 (2000) 735–741.

[11] R. Rübenhagen, S. Morbach, R. Krämer, The osmoreactive betaine carrier BetP from *Corynebacterium glutamicum* is a sensor for cytoplasmic K^+, EMBO J. 20 (2001) 5412–5420.

[12] C. Ziegler, S. Morbach, D. Schiller, R. Krämer, C. Tziatzios, D. Schubert, W. Kühlbrandt, Projection structure and oligomeric state of the osmoregulated sodium/-glycine betaine symporter BetP of *Corynebacterium glutamicum*, J. Mol. Biol. 337 (2004) 1137–1147.

[13] S. Ressl, T. Van Scheltinga, C. Vonrhein, V. Ott, C. Ziegler, Molecular basis of regulation and Na^+-coupled transport in the glycine-betaine symporter BetP, Nature 458 (2009) 47–53.

[14] C. Ziegler, E. Bremer, R. Kraemer, The BCCT family of carriers: from physiology to crystal structure, Mol. Microbiol. 78 (2010) 13–34.

[15] C. Altenbach, S.L. Flitsch, H.G. Khorana, W.L. Hubbell, Structural studies on transmembrane proteins. 2. Spin labelling of bacteriorhodopsin mutants at unique cysteines, Biochemistry 28 (1989) 7806–7812.

[16] C. Altenbach, T. Marti, H.G. Khorana, W.L. Hubbell, Transmembrane protein structure: spin labeling of bacteriorhodopsin mutants, Science 248 (1990) 1088–1092.

[17] J.P. Klare, H.-J. Steinhoff, Spin labeling EPR, Photosynth. Res. 102 (2009) 377–390.

[18] W.L. Hubbell, C. Altenbach, Investigation of structure and dynamics in membrane proteins using site-directed spin labeling, Curr. Opin. Struct. Biol. 4 (1994) 566–573.

[19] W.L. Hubbell, D.S. Cafiso, C. Altenbach, Identifying conformational changes with site-directed spin labeling, Nat. Struct. Biol. 7 (2000) 735–739.

[20] E. Bordignon, H.J. Steinhoff, ESR spectroscopy in membrane biophysics, in: M.A. Hemminga, L.J. Berliner (Eds.), Biological Magnetic Resonance, Vol. 27, Springer-Verlag GmbH, Heidelberg, 2007, pp. 129–164.

[21] W.L. Hubbell, A. Gross, R. Langen, M.A. Lietzow, Recent advances in site-directed spin labeling of proteins, Curr. Opin. Struct. Biol. 8 (1998) 649–656.

[22] M. Pfeiffer, T. Rink, K. Gerwert, D. Oesterhelt, H.J. Steinhoff, Site-directed spin-labeling reveals the orientation of the amino acid side-chains in the E–F loop of bacteriorhodopsin, J. Mol. Biol. 287 (1999) 163–171.

[23] E. Perozo, D.M. Cortes, L.G. Cuello, Three-dimensional architecture and gating mechanism of a K^+ channel studied by EPR spectroscopy, Nat. Struct. Biol. 5 (6) (1998) 459–469.

[24] A.A. Wegener, J.P. Klare, M. Engelhard, H.J. Steinhoff, Structural insights into the early steps of receptor–transducer signal transfer in archaeal phototaxis, EMBO J. 20 (2001) 5312–5319.

[25] D. Hilger, H. Jung, E. Padan, C. Wegener, K.P. Vogel, H.J. Steinhoff, G. Jeschke, Assessing oligomerization of membrane proteins by four-pulse DEER: pH-dependent dimerization of NhaA Na^+/H^+ antiporter of *E. coli*, Biophys. J. 89 (2005) 1328–1338.

[26] S.N. Cohen, A.C.Y. Chang, L. Hsu, Nonchromosomal antibiotic resistance in bacteria: genetic transformation of *Escherichia coli* by R-factor DNA, Proc. Natl. Acad. Sci. U. S. A. 69 (1972) 2110–2114.

[27] W. Schaffner, C. Weissmann, A rapid, sensitive and specific method for the determination of protein in dilute solution, Anal. Biochem. 56 (1973) 502–514.

[28] K.I. Racher, D.E. Culham, J.M. Wood, Requirements for osmosensing and osmotic activation of transporter ProP from *E. coli*, Biochemistry 40 (2001) 7324–7333.

[29] C. Altenbach, D.A. Greenhalgh, H.G. Khorana, W.L. Hubbell, A collision gradient method to determine the immersion depth of nitroxides in lipid bilayers: application to spin-labeled mutants of bacteriorhodopsin, Proc. Natl. Acad. Sci. U. S. A. 91 (1994) 1667–1671.

[30] D. Schiller, R. Krämer, S. Morbach, Cation specificity of osmosensing by the betaine carrier BetP of *Corynebacterium glutamicum*, FEBS Lett. 563 (2004) 108–112.

[31] R.E. Martin, M. Pannier, F. Diederich, V. Gramlich, M. Hubrich, H.W. Spiess, Determination of end-to-end distances in a series of TEMPO diradicals of up to 2.8 nm length with a new four-pulse double electron electron resonance experiment, Angew. Chem. Int. Ed. 37 (1998) 2833–2837.

[32] M. Pannier, S. Veit, A. Godt, G. Jeschke, H.W. Spiess, Dead-time free measurement of dipole–dipole interactions between electron spins, J. Magn. Reson. 142 (2000) 331–340.

[33] G. Jeschke, Y. Polyhach, Distance measurements on spin-labeled biomacromolecules by pulsed electron paramagnetic resonance, Phys. Chem. Chem. Phys. 9 (2007) 1895–1910.

[34] C. Beier, H.J. Steinhoff, A structure-based simulation approach for electron paramagnetic resonance spectra using molecular and stochastic dynamics simulations, Biophys. J. 91 (2006) 2647–2664.

[35] G. Jeschke, C. Wegener, M. Nietschke, H. Jung, H.J. Steinhoff, Inter-residual distance determination by four-pulse DEER in an integral membrane protein: the Na^+/proline transporter PutP of *Escherichia coli*, Biophys. J. 86 (2004) 2551–2557.

[36] G. Jeschke, V. Chechik, P. Ionita, A. Godt, H. Zimmermann, J. Bahman, C.R. Timmel, D. Hilger, H. Jung, Deer Analysis 2006 — a comprehensive software package for analyzing pulsed ELDOR data, Appl. Magn. Reson. 30 (2006) 473–498.

[37] B. Poolman, J.J. Spitzer, J.M. Wood, Bacterial osmosensing: roles of membrane structure and electrostatics in lipid–protein and protein–protein interactions, Biochim. Biophys. Acta 166 (2004) 88–104.

[38] H. Peter, A. Burkovski, R. Krämer, Osmo-sensing by N- and C terminal extensions of the glycine betaine uptake system BetP of *Corynebacterium glutamicum*, J. Biol. Chem. 273 (1998) 2567–2574.

[39] C. Altenbach, A.K. Kusnetzow, O.P. Ernst, K.P. Hofmann, W.L. Hubbell, High-resolution distance mapping in rhodopsin reveals the pattern of helix movement due to activation, Proc. Natl. Acad. Sci. U. S. A. 105 (2008) 7439–7444.